Hydrodynamic Shifts in the NMR Spectrum of ^{3}He-B

J. Hutchins, D. F. Brewer, and D. Kruppa
Physics Laboratory, University of Sussex, Brighton, Sussex BN1 9QH, United Kingdom
(Received 8 July 1985)

We have measured the flow-induced shift in the NMR spectrum of ^{3}He-B. Above a temperature-independent critical velocity, the absorption line is observed to shift to higher frequencies as the flow is increased, in qualitative agreement with the theory of textural deformation in the presence of flow due to Fetter.

PACS numbers: 67.50.Fi

In previously reported work[1-5] we investigated both the ac and dc flow properties of superfluid ^{3}He through a parallel-plate superleak of plate separation 48 μm. In those experiments we used a gold-plated flexible plastic diaphragm to drive and detect superflow electrically. We have now constructed a new flow cell in order to extend these measurements to persistent current and NMR experiments. The results of our persistent-current experiments will be published elsewhere. In this paper we will concentrate on low-pressure (5-bar) measurements of the transverse NMR adsorption in the presence of superflow.

NMR on flow can be used to determine the orientational effect of superflow on the B-phase $\hat{\mathbf{n}}$ texture. It also yields information on the relative magnitudes of the competing terms in the Ginsburg-Landau free energy expansion, as discussed below, and the flow-induced shift can be related to the longitudinal resonance frequency.

The cell consists of a copper vessel with two separate volumes, each containing copper sinter and having a number of access ports. The diaphragm assembly bolts onto the top of this cell, the two sides of the diaphragm connecting through copper tubes to the two different volumes. Hydrodynamic flow can hence be generated in any geometry connecting the two sinter volumes via ports beneath the heat exchanger. In the present work we have as this geometry two superleaks in parallel connecting the two volumes. The superleaks are both parallel plates separated by 100 μm, but they differ in their lengths by a factor of 20 (1 and 20 mm). The diaphragm assembly consists as before[2] of a gold-plated Mylar diaphragm with two capacitor plates positioned on either side of it. The voltage between one side of the diaphragm and the electrode facing it is then ramped in such a way as to produce a steady dc flow in the superleaks.[5] This mass flow is then measured by monitoring the capacitance between the other side of the diaphragm and the other electrode. The NMR coil used in the experiments reported in this paper is wound around one of the connecting channels, of internal diameter 2 mm, between the two superleaks. The static NMR field of 278 G is applied perpendicular to the axis of the coil and hence is also perpendicular to the superflow. The transverse absorption is observed by modulation of the static NMR field and detected by a standard Q-meter spectrometer. The field sweep is calibrated by our changing the rf drive frequency in the normal Fermi liquid and measuring the corresponding shift in the absorption line. For thermometry, we measure the frequency of superfluid oscillations generated in the superleaks,[1,2] which we calibrate against a pulsed platinum NMR thermometer. This means that we are not constrained by the platinum thermometer to work at any particular magnetic field, although all the data presented in this paper were obtained at 278 G. The sample is cooled into the superfluid phases by a standard copper nuclear refrigerator.

A given voltage ramp, $V^2\propto$ time, generates a certain superfluid mass current $J_s=\rho_s v_s$, rather than a certain superfluid velocity v_s. Hence we normally adopt the method of keeping J_s constant on a given experimental run. The transverse absorption is then measured both in the absence and in the presence of a superflow during slow warming in the B phase. These two NMR absorption lines are then compared in order to determine the flow-induced shift.

In the absence of superflow the equilibrium texture is determined by the competition between four orientational energies, namely, the two surface anisotropy energies, the bulk bending energy, and the bulk field energy (see, for example, Brinkman and Cross[6]). The characteristic length[6] $R_c\simeq(20\text{ cm G})(1-T/T_c)H^{-1}$ defines the distance over which the $\hat{\mathbf{n}}$ vector adopts its bulk equilibrium configuration in the field, $\mathbf{H}$, after being perturbed by the surface. For $H=278$ G, the surface anisotropy energy dominates over the surface dipole energy and therefore determines the orientation of $\hat{\mathbf{n}}$ at the surface. For distances greater than R_c from the surface, the bulk field energy orients $\hat{\mathbf{n}}$ parallel to $\mathbf{H}$. Whenever $\hat{\mathbf{n}}$ makes a finite angle, θ, with $\mathbf{H}$, the transverse absorption shifts to higher frequencies according to the equation[7]

$$\omega_t^2=\omega_L^2+\Omega_B^2\sin^2\theta,$$

where ω_L and Ω_B are the Larmor and longitudinal frequencies, respectively.

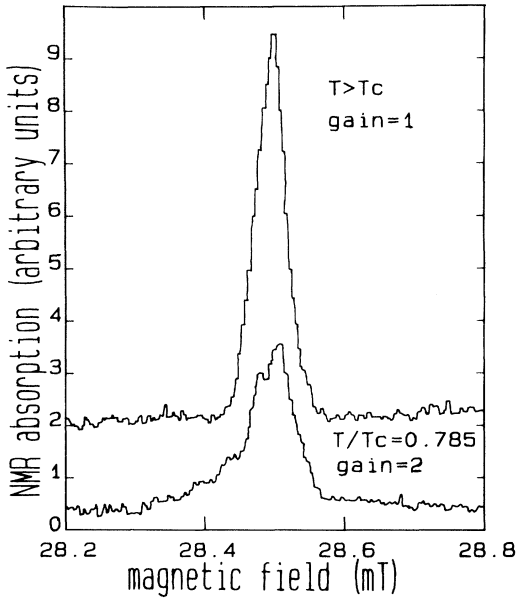

FIG. 1. Transverse NMR absorption lines in the absence of flow. The superfluid absorption line shows a well-developed high-frequency tail.

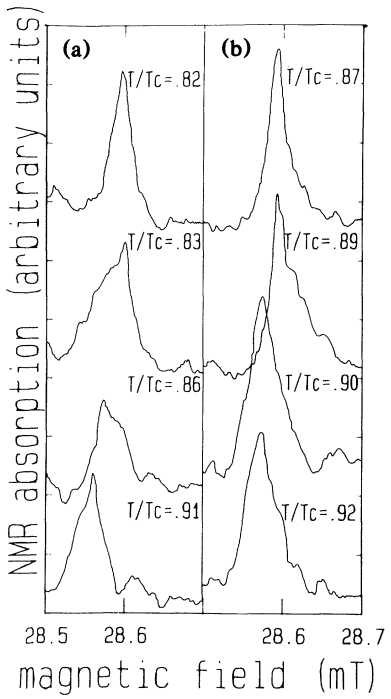

FIG. 2. Transverse absorption in the presence of superflows of (a) $J_s = 1.66 \times 10^{-4}$ g/cm^2 and (b) $J_s = 1.03 \times 10^{-4}$ g/cm^2 · sec. The line shapes are explained in the text.

Just below T_c the transverse absorption is essentially identical to that observed in the normal Fermi liquid. The magnetic healing length, R_c, is small in comparison to the NMR tube diameter, and the $\hat{\mathbf{n}}$ texture is almost uniformly aligned parallel to the static field in the bulk of the sample. As the temperature is reduced, R_c grows and a high-frequency (low-field) tail is observed corresponding to regions where $\theta \neq 0$. This is shown in Fig. 1, which is a graph of the signal-averaged transverse absorption observed in the absence of a flow in the normal Fermi liquid and at $T/T_c = 0.785$. The orientation that $\hat{\mathbf{n}}$ adopts at the surface depends on the direction of $\mathbf{H}$ relative to the surface. In fact, if the angle that $\mathbf{H}$ makes with the surface is sufficiently large, there are two minima in the free energy, probably corresponding to the double-peaked structure observed in Fig. 1.

Typical sets of flow-shifted data are shown in Fig. 2. At low temperatures ($T/T_c < 0.82$), the absorption line is virtually identical to that in the absence of a flow. As the temperature is increased, the NMR line shifts to higher frequencies and shows substantial broadening at the highest mass currents. Figure 3 shows the temperature dependence of this hydrodynamic frequency shift at a number of mass currents. The origin of the temperature dependence and line shape in the presence of flow can be understood within the framework of a theory of NMR of ^{3}He-B in the presence of superflow due to Fetter.[8]

Using a Ginzburg-Landau free-energy expansion and weak-coupling theory, Fetter derives the effect of superflow on the equilibrium configuration of ^{3}He-B. Leggett's equations[9] are then solved in order to determine the effect on the NMR spectrum. Fetter's solution for the transverse resonance in the strong-field limit, $G_z H^2 >> Kq^2$ and $>> G_d$ (where G_z, K, and G_d are the coupling constants for the magnetic field, flow, and nuclear-dipole terms in the free-energy expansion,

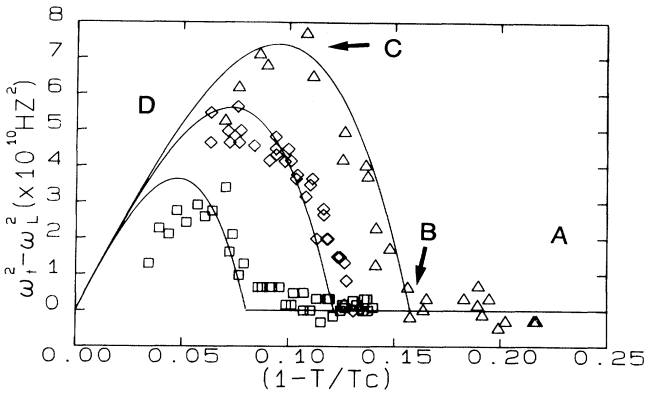

FIG. 3. Flow-induced frequency shifts as a function of $(1 - T/T_c)$ at various mass currents. Squares, 6.45×10^{-5} g/cm^2 · sec; lozenges, 1.03×10^{-4} g/cm^2 · sec; triangles, 1.40×10^{-4} g/cm^2 · sec. The solid curves are calculations from Fetter's theory. The lettered regions are explained in the text.

and $\hbar q/2m = v_s$) is

$$\omega_t^2 = \omega_L^2 + \tfrac{4}{5}\Omega_B^2(1-\cos\phi),$$

where ϕ is the solution of

$$\phi = \begin{cases} 0, & 2kq^2/G_D < 1, \\ \arccos(G_D/2Kq^2), & 2Kq^2/G_d > 1. \end{cases}$$

The velocity dependence of the shift is then carried in ϕ. Fetter's theory predicts that for $2Kq^2/G_D < 1$ no flow-induced shifts occur. For $2Kq^2/G_D > 1$, the transverse absorption shifts to high frequencies, rapidly saturating at $\omega_t^2 = \omega_L^2 + \frac{4}{5}\Omega_B^2$ as v_s is increased.

Brinkman and Cross[6] have adopted a different (but equivalent) approach to the same problem. They treat the various orientational forces on $\hat{\mathbf{n}}$ as perturbations on the B-phase order parameter. This perturbative approach leads to an orientational energy of the form

$$\Delta E \propto \left[\left(\hat{\mathbf{n}}\cdot\frac{\mathbf{H}}{H_c}\right)^2 + \frac{2}{5}\left(\frac{\mathbf{v}_s}{v_c}\cdot\mathbf{R}\cdot\frac{\mathbf{H}}{H_c}\right)^2 + \left(\hat{\mathbf{n}}\cdot\frac{\mathbf{v}_s}{v_c}\right)^2\right],$$

where at $H = H_c$ and $v_s = v_c$, $2Kq^2 = G_z H^2 = G_d$ in Fetter's notation, and $\mathbf{R}$ is the usual rotation matrix of the spin variables relative to the orbital variables.

The general features of Fig. 3 can now be understood. In region A the superfluid density is sufficiently large that v_s is below its critical value of $v_c = (\hbar/2m)(G_d/k)$, and no flow-induced shifts occur. At point B, the superfluid density was decreased with increasing temperature, v_s has reached its critical value, v_c, and the transverse absorption rapidly shifts to higher frequencies. At point C, v_s has increased sufficiently that the shift has saturated at $\omega_t^2 = \omega_L^2 + \frac{4}{5}\Omega_B^2$. In region D the shift is decreasing since $\Omega_B^2 \propto (1 - T/T_c)$.

With our experimental dimensions, we would expect substantial deviations from the uniform textures of Fetter due to the orientational effect of boundaries. This is observed in the flow-shifted line shapes depicted in Fig. 2, which shows two sets of NMR data. At the comparatively high mass current of $J_s = 1.66 \times 10^{-4}$ g/cm$^2\cdot$sec, the critical velocity is reached at $T/T_c = 0.83$, when the temperature-dependent healing length is comparatively long, $R_c \simeq 0.3$ mm. A proportion of the absorption line shifts to higher frequencies corresponding to the contribution from the central region of the NMR tube, while the absorption remains peaked at ω_L. As the reduced temperature increases, R_c decreases, and a high-frequency peak develops which we associate with the textural configuration determined by Fetter's bulk model. Figure 2 also shows a set of flow-shifted data taken at a lower mass current of $J_s = 1.032 \times 10^{-4}$ g/cm$^2\cdot$sec. Here v_c is reached at $T/T_c = 0.9$ when $R_c = 0.2$ mm, and no substantial broadening is observed.

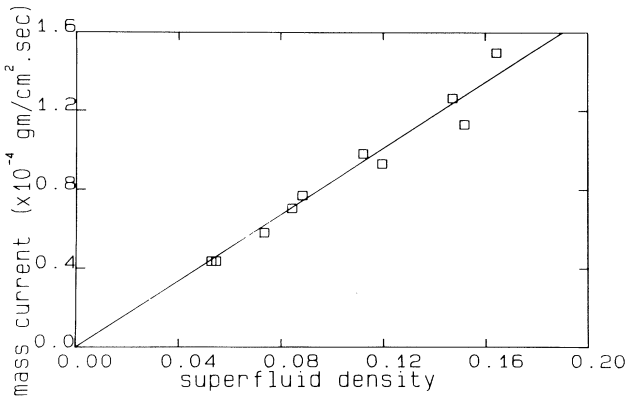

FIG. 4. The critical velocity for transverse frequency shifts at 278 G. The solid curve is a least squares fit to the data and gives $v_c = 0.1$ mm/sec.

Fetter's theory predicts a critical velocity of 0.32 mm/sec at 5 bars, independent of temperature. We have used Archie's[10] superfluid-density data to determine the superfluid densities at which the frequency shift occurs and plotted this against mass current in Fig. 4. The data clearly show that v_c is temperature independent at $v_c = 0.10$ mm/sec, if we assume no dissipation in the superflow. Figure 4 is also consistent with this assumption since no significant deviations from linearity are observed at the highest mass currents. Within the framework of Fetter's theory, these results show that, at 5 bars, the relative magnitudes of the coupling constants K and G_D are $2Kq^2/G_D = 1$ at $v_s = 10^{-2}$ cm/sec and at 278 G. This should be compared to the weak-coupling prediction of $2Kq^2/G_D = 1$ at 3.5×10^{-2} cm/sec.

Fetter's theory also predicts a maximum frequency shift determined by Ω_B^2. Ahonen, Krusius, and Paalanen[11] have measured the temperature dependence of the longitudinal resonance at 18.7 bars. They find $\Omega_B^2 = 3.95 \times 10^{12}(1 - T/T_c)$ Hz^2. Weak coupling predicts a decrease in the longitudinal resonance frequency by a factor of 0.35 between 18.7 and 5 bars. The curves in Fig. 3 are calculated from Fetter's theory with $v_c = 0.10$ mm/sec and the Helsinki longitudinal frequency determination scaled by the above weak-coupling factor. The good agreement obtained with our experimental results indicates that strong-coupling corrections to Ω_B^2 are insignificant over this wide pressure range.

Flint, Muller, and Adams[12] have also investigated NMR in flowing superfluid ^{3}He using a double Pomeranchuk cell arrangement. While various flow-induced effects were seen in the A phase, no flow-induced shifts were observed in the B phase for $v_s \lesssim 1$ mm/sec. On the melting curve Fetter's theory predicts $v_c = 1.05$ mm/sec. The likely presence of solid in the flow channel, however, makes the deter-

mination of flow velocities open to uncertainty.

Preliminary data taken at 18.7 bars are also in broad agreement with Fetter's theory in that the transverse frequency shift is substantially larger ($\omega_t^2-\omega_L^2=10^{11}$ Hz^2 at $T/T_c=0.96$ and $J_s=9\times10^{-5}$ g/cm$^2\cdot$sec) than that observed in the 5-bar data. This is due to the pressure-dependent increase in Ω_B^2. The analysis of these high-pressure data is complicated by the presence of asymmetries in the NMR shift with respect to the flow direction. This may be due to persistent currents or it may be textural in origin. Experimental work is continuing in order to elucidate these and other phenomena.

In conclusion, we have made experimental measurements of the predicted hydrodynamic NMR frequency shift in ^{3}He-B at low pressure. We have found broad agreement with the theory of Fetter, in that the transverse absorption is observed to shift to higher frequencies above a temperature-independent critical velocity. The shift rapidly saturates at a frequency determined by the longitudinal frequency as the superfluid velocity is increased. The magnitude of the critical velocity determines the relative magnitude of the coupling constants K and G_D as $2Kq^2/G_D=1$ at $v_s=10^{-2}$ cm/sec and at 278 G. This value of v_s is a factor 3.5 smaller than the theoretical value assuming weak coupling.

We would like to thank A. J. Leggett for helpful discussions, and C. A. Mills, whose technical expertise made this work possible. This work was carried out under Science and Engineering Research Council Grants No. GR/B/65137 and No. GR/D/12040, and in part under Grant No. B/SF/122 (D.F.B., Senior Fellowship).

[1]A. J. Dahm, D. S. Betts, D. F. Brewer, J. D. Hutchins, J. Saunders, and W. S. Truscott, Phys. Rev. Lett. **45**, 1411 (1980).

[2]J. D. Hutchins, D.Phil. thesis, University of Sussex, 1980 (unpublished).

[3]J. D. Hutchins, D. S. Betts, D. F. Brewer, A. J. Dahm, and W. S. Truscott, Physica **108B**, 1139 (1981).

[4]Ren-Zhi Ling, D. S. Betts, and D. F. Brewer, Phys. Rev. Lett. **53**, 930 (1984).

[5]Ren-Zhi Ling, D.Phil. thesis, University of Sussex, 1984 (unpublished).

[6]W. F. Brinkman and M. W. Cross, in *Progress in Low Temperature Physics,* edited by D. F. Brewer (North-Holland, Amsterdam, 1978), Vol. 7A.

[7]W. F. Brinkman, H. Smith, D. D. Osheroff, and E. I. Blount, Phys. Rev. Lett. **33**, 624 (1974).

[8]A. L. Fetter, J. Low Temp. Phys. **23**, 245 (1976).

[9]A. J. Leggett, Rev. Mod. Phys. **47**, 331 (1975).

[10]C. N. Archie, Ph.D. thesis, Cornell University, 1978 (unpublished).

[11]A. I. Ahonen, M. Krusius, and M. A. Paalanen, J. Low Temp. Phys. **25**, 421 (1976).

[12]E. B. Flint, R. M. Muller, and E. D. Adams, J. Low Temp. Phys. **33**, 43 (1978).